WHEN IS A MAXIMAL INVARIANT HYPOTHESIS TEST BETTER THAN THE GLRT?

Hyung Soo Kim and Alfred O. Hero

Department of Electrical Engineering and Computer Science
University of Michigan, Ann Arbor, MI 48109-2122

ABSTRACT

There has been considerable recent interest in applying maximal invariant (MI) hypothesis testing as an alternative to the generalized likelihood ratio test (GLRT). This interest has been motivated by several attractive theoretical properties of MI tests including: exact robustness to variation of nuisance parameters, finite-sample min-max optimality (in some cases), and distributional robustness, i.e. insensitivity to changes in the underlying probability distribution over a particular class. Furthermore, in some important cases the MI test gives a reasonable test while the GLRT has worse performance than the trivial coin flip decision rule [1]. However, in other cases, like the deep hide target detection problem, there are regimes (SNR, number of wireless users, coherence bandwidth) for which either of the MI and the GLRT can outperform the other. We will discuss conditions under which the MI tests can be expected to outperform the GLRT in the context of a radar imaging and target detection application.

1. INTRODUCTION

In automatic target recognition, the most important issue is reliable detection which is robust to target and clutter variability, yet maintains the highest possible discrimination capability. In the past, most adaptive radar and array detection problems have been formulated under the general assumption that the target has known form but unknown amplitude in Gaussian noise whose covariance matrix is totally unknown or unstructured. The nature of this assumption led to the application of the general multivariate analysis of variance (GMANOVA) model [2] to the measurements, and the subsequent development of many detection algorithms. With this assumption and the GMANOVA model, Kelly [3] derived the constant false alarm rate (CFAR) test using the generalized likelihood ratio (GLR) principle.

However, when a prior structure of the clutter covariance matrix exists, one can expect an improvement in performance by exploiting this a priori structure. Also when

tractable, the reduced parameterization of the structured covariance can be introduced and the GLR test can be applied. For adaptive arrays, Bose and Steinhardt [4] proposed an MI detector which outperforms the Kelly's test when the clutter covariance matrix is assumed to have a certain known block diagonal structure. This work was the springboard in [5] for synthetic aperture radar (SAR) imaging target detection in the difficult deep hide scenario where the target parks along a known boundary separating two adjacent clutter regions. Indeed, under the assumption that the two clutter types are statistically independent, the spatial covariance has a similar block diagonal structure to that in [4] and this structure was used in [5] to derive another MI test.

In this paper we extend the work reported in [5] by deriving the form of the GLR test and comparing the invariant methods of [4] and [5]. Derivations of the GLR and MI test statistics for the case of structured covariance are not trivial, and the details are omitted due to space limitations. Here we compare the GLR tests to the MI tests on the basis of simulation for the deep hide scenario when the boundary can be accurately estimated. We establish that the MI test outperforms the GLRT when the target-to-clutter ratio is low.

2. GLR VS. INVARIANCE PRINCIPLES

Fig. 1 displays the magnitude of a complex valued SAR clutter image of a rural scene consisting of two clutter types (forest canopy and grass field) separated by a boundary. The deep hide target detection problem treated in this paper is to detect a target that straddles the boundary between regions A and B. We make the assumptions that the complex clutter image is circular Gaussian with zero mean and that two spatial samples taken respectively from region A and region B are uncorrelated. By centering a 1-pixel wide vertical window with fixed vertical extent at the boundary (or its estimate) in Fig. 1 and sliding it over the image from left to right we obtain a reduced image (Fig. 10) with a horizontal boundary. Any of the vectors repacked from the clutter-alone image chips shown in Fig. 10 will be multivariate complex Gaussian with zero mean and covariance matrix R having block diagonal structure. Then by con-

401

catenating these vectors we obtain the measurement $\mathbf{X} =$
$[\underline{x}_1, \dots, \underline{x}_n]$:

$$\mathbf{X} = a\,\underline{s}\,\underline{b}^H + \mathbf{N}$$

where $\underline{s}$ is the n-dimensional target signature with unknown amplitude a, $\underline{b}$ is the target location vector, and $vec(\mathbf{N}) \sim \mathcal{CN}(\underline{0}, \mathbf{R} \otimes \mathbf{I}_n)$, i.e. $\mathbf{N}$ follows a multivariate zero-mean complex normal distribution with covariance $\mathbf{R} \otimes \mathbf{I}_n$. Note that if $\underline{b}^H = [1, 0, \dots, 0]$, the first column $\underline{x}_1$ is the primary data which may contain the target. The goal is to construct a test that a given chip contains clutter alone (H_0) vs. clutter plus target (H_1) where target spatial structure is known. We separate the clutter scenarios into three different cases:

- Case 1: $\mathbf{R} = \begin{bmatrix} \mathbf{R}_A & \mathbf{O} \\ \mathbf{O} & \mathbf{R}_B \end{bmatrix}$
(totally unknown clutter in regions A and B)

- Case 2: $\mathbf{R} = \begin{bmatrix} \mathbf{R}_A & \mathbf{O} \\ \mathbf{O} & \sigma^2\mathbf{I} \end{bmatrix}$
(clutter known in region B up to variance σ^2)

- Case 3: $\mathbf{R} = \begin{bmatrix} \mathbf{R}_A & \mathbf{O} \\ \mathbf{O} & \mathbf{I} \end{bmatrix}$
(clutter known exactly in region B)

where $\mathbf{R}_A > 0$, $\mathbf{R}_B > 0$, and $\sigma^2 > 0$.

Since there exists no uniformly most powerful test for these structured covariance matrices, the invariance principle can be applied in addition to the GLR method as good candidates for sub-optimal CFAR tests. It can be shown that in the case of real observations the GLR is closed form while in the complex case the GLR has explicit form up to rooting a complex quartic equation in the complex target amplitude parameter a. GLR test statistics are listed in Table 1 where the measurement matrix is partitioned as

$$\mathbf{X} = \begin{bmatrix} \mathbf{X}_A \\ \mathbf{X}_B \end{bmatrix} = \begin{bmatrix} \underline{x}_{A1} & \mathbf{X}_{A2} \\ \underline{x}_{B1} & \mathbf{X}_{B2} \end{bmatrix}$$

and each column corresponds to pixel values in a different chip. The known target signature is $\underline{s} = \begin{bmatrix} \underline{s}_A^H & \underline{s}_B^H \end{bmatrix}^H$, and

$$p(a, \mathbf{X}_A) = (\underline{x}_{A1} - a\underline{s}_A)^H (\mathbf{X}_{A2}\mathbf{X}_{A2}^H)^{-1}(\underline{x}_{A1} - a\underline{s}_A)$$

$$q(a, \mathbf{X}_B) = tr\{(\mathbf{X}_B - a\underline{s}_B\underline{e}_1^T)^H (\mathbf{X}_B - a\underline{s}_B\underline{e}_1^T)\}.$$

Here the subscripts denote the two different regions A and B. $\underline{x}_{A1}(m_A \times 1)$ and $\underline{x}_{B1}(m_B \times 1)$ denote pixels in the chip which is being tested for containing the target.

As described in [2], the MI test is constructed by applying the likelihood ratio test to a statistic called the maximal invariant. The maximal invariant is the lowest dimension statistic summarizing the data yet preserving target vs. clutter discrimination capability for the specific parameter uncertainty. Using the maximal invariant approach, Bose and

$\mathbf{R}_A$	$\mathbf{R}_B$	Log GLR : $\frac{1}{n}\ln\Lambda = \max_a\{\cdot\}$	
?	?	$\ln\left[\dfrac{1+p(0,\mathbf{X}_A)}{1+p(a,\mathbf{X}_A)}\right]$	$+\ln\left[\dfrac{1+p(0,\mathbf{X}_B)}{1+p(a,\mathbf{X}_B)}\right]$
?	$\sigma^2\mathbf{I}$	$\ln\left[\dfrac{1+p(0,\mathbf{X}_A)}{1+p(a,\mathbf{X}_A)}\right]$	$+\,m_B\cdot\ln\left[\dfrac{q(0,\mathbf{X}_B)}{q(a,\mathbf{X}_B)}\right]$
?	$\mathbf{I}$	$\ln\left[\dfrac{1+p(0,\mathbf{X}_A)}{1+p(a,\mathbf{X}_A)}\right]$	$+\frac{1}{n}[q(0,\mathbf{X}_B)-q(a,\mathbf{X}_B)]$

Table 1. GLR tests for Case 1, 2 and 3. (The notation '?' denotes 'unknown' quantity in the model)

Steinhardt [4] derived an MI test for Case 2, and modified the Kelly's test [3] to fit Case 1. However, using a different function of the maximal invariant we have obtained another MI test for each case which reduces exactly to the unstructured GLR test when a target is entirely contained in one of regions A or B. The MI tests are listed in Table 2 where

$$q_A = 1 + \underline{x}_{A1}^H(\mathbf{X}_{A2}\mathbf{X}_{A2}^H)^{-1}\underline{x}_{A1} \quad , \quad v_2 = \frac{tr\{\mathbf{X}_B^H\mathbf{X}_B\}}{m_B}$$

$$q_B = 1 + \underline{x}_{B1}^H(\mathbf{X}_{B2}\mathbf{X}_{B2}^H)^{-1}\underline{x}_{B1} \quad , \quad v_3 = n.$$

$\mathbf{R}_A$	$\mathbf{R}_B$	$\dfrac{\left[\begin{smallmatrix}\underline{s}_A^H & \underline{s}_B^H\end{smallmatrix}\right]\begin{bmatrix}\mathbf{K}_A & \mathbf{O} \\ \mathbf{O} & \mathbf{K}_B\end{bmatrix}^{-1}\begin{bmatrix}\underline{x}_{A1} \\ \underline{x}_{B1}\end{bmatrix}\Big|^2}{\left[\begin{smallmatrix}\underline{s}_A^H & \underline{s}_B^H\end{smallmatrix}\right]\begin{bmatrix}\mathbf{K}_A & \mathbf{O} \\ \mathbf{O} & \mathbf{K}_B\end{bmatrix}^{-1}\begin{bmatrix}\underline{s}_A \\ \underline{s}_B\end{bmatrix}}$
?	?	$\mathbf{K}_A = q_A\mathbf{X}_{A2}\mathbf{X}_{A2}^H, \quad \mathbf{K}_B = q_B\mathbf{X}_{B2}\mathbf{X}_{B2}^H$
?	$\sigma^2\mathbf{I}$	$\mathbf{K}_A = q_A\mathbf{X}_{A2}\mathbf{X}_{A2}^H, \quad \mathbf{K}_B = v_2\mathbf{I}$
?	$\mathbf{I}$	$\mathbf{K}_A = q_A\mathbf{X}_{A2}\mathbf{X}_{A2}^H, \quad \mathbf{K}_B = v_3\mathbf{I}$

Table 2. MI tests for Case 1, 2 and 3

3. NUMERICAL COMPARISONS

To compare the performance of the GLR and MI tests derived under the three structured covariance assumptions, ROC curves are generated for each case. In Figs. 2-4, 8 different tests are compared case by case: structured Kelly's test matched to Case 1, Bose and Steinhardt's test matched to Case 2, and the three MI tests and the three GLRTs matched to one of the three cases. In all cases, these figures confirm that the tests derived under the matched assumption outperform those which are mismatched.

Of particular interest, however, are the crossings in the low probability of false alarm (P_{FA}) regions between the GLR tests and the MI tests. In Fig. 2, we can observe the gains in probability of detection (P_D) of MI test 1 over GLRT 1 for $P_{FA} < 0.1$. Moreover, it should be noted that the structured Kelly's test is outperformed by MI test 1 in low P_{FA} and by GLRT 1 in high P_{FA}. Also in Case 2 (Fig. 3), both MI test 2 and GLRT 2 outperform Bose and Steinhardt's matched test and it appears that MI test 2 slightly

402

outperforms GLRT 2 for low P_{FA}. These observations also hold for mismatched cases: between MI test 1 and GLRT 1 in Case 2/3 (Figs. 3/4), and between MI test 2 and GLRT 2 in Case 1 (Figs. 2). For Case 3 (Fig. 4), the ROC curve for GLRT 2 approaches that of the matched GLRT 3 since large number of pixels ($m_B n = 60 \times 61$) provide sufficiently accurate estimates of the variance in region B.

In Figs. 5 and 7, ROC curves are compared with different ratios of m_A/m_B from those of Figs. 2-4. Kelly's test for Case 1 and Bose and Steinhardt's test for Case 2 are shown to be more sensitive to the dimensional parameters m_A and m_B.

The relative advantages of MI vs. GLR tests are more closely investigated in Fig. 6 and 8. In (a) of both figures, we increased n while fixing SNR. Note that the GLR and MI tests have ROCs which are virtually indistinguishable for large n. In (b), however, by increasing SNR while fixing n, the P_{FA} positions of the crossings of the ROCs for the GLR and MI tests decreased. In particular, if one fixes a level of false alarm, say $P_{FA} = 0.1$, then note from Fig. 6 (b) that the GLR test dominates the MI test for SNR = 19dB while the reverse is true for SNR = 7dB.

Next, we consider an application to real SAR imagery in Fig. 1. The image shown is a rural scene near Redstone Arsenal at Huntsville, Alabama, reproduced from the data collected using the Sandia National Laboratories Twin Otter SAR sensor payload operating at X band. The boundary was hand extracted and a 9 × 7 SLICY target extracted from Fig. 9 (e) was inserted so that it straddles the boundary. The images in Fig. 9 correspond to the same target but viewed at different pose angles of azimuth. The data from which these images are reproduced was downloaded from the MSTAR SAR database at the Center for Imaging Science (www.cis.jhu.edu). With the realigned image in Fig. 10, structured Kelly's test, MI test 1, and GLRT 1 statistics are calculated and maximized over each possible location along the boundary. Table 3 shows the minimum magnitude of amplitude required for each test to detect the target at the correct location. In this experiment both the GLR and MI tests perform as good as the structured Kelly's test.

Test	$|a|$
Structured Kelly	1.407×10^{-2}
MI Test 1	1.454×10^{-2}
GLRT 1	1.462×10^{-2}

Table 3. Amplitudes required in magnitude for detection of the target at the correct location.

Finally, we maximized the test statistics over the different target poses in Fig. 9 as well as over all possible locations along the boundary. Only the peak values for 9 target signatures are plotted in Fig. 11, and all the tests successfully picked the signature at the true pose and location.

4. CONCLUSION

The deep hide scenario considered in this paper complicates the design of optimal target detectors. This scenario gives rise to block diagonal constraints imposed by the clutter covariance structure. Both GLR and MI tests can be derived under these constraints. Numerical results indicate that neither GLR nor MI tests dominate the other in terms of ROC performance. The GLRT outperforms the MI test only when high estimator accuracy is attainable, e.g. for a large number of samples, but otherwise MI test is better especially in low P_{FA}. Therefore, MI test not only plays an important role as an alternative to GLRT, but also has the desirable property of reliable performance in low P_{FA} with a small number of snapshots. The results in this paper are generalizable to other applications where invariance principle can be applied.

5. REFERENCES

[1] E. L. Lehmann, *Testing Statistical Hypotheses*, Wiley, New York, 1959.

[2] T. Kariya and B. K. Sinha, *Robustness of Statistical Tests*, Academic Press, San Diego, 1989.

[3] E. J. Kelly, "An adaptive detection algorithm," *IEEE Trans. Aerosp. Electron. Syst.*, vol. AES-22, pp. 115-127, Mar. 1986.

[4] S. Bose and A. O. Steinhardt, "A maximal invariant framework for adaptive detection with structured and unstructured covariance matrices," *IEEE Trans. Sig. Proc.*, vol. 43, no. 9, pp. 2164-2175, Sep. 1995.

[5] A. O. Hero and C. Guillouet, "Robust detection of SAR/IR targets via invariance," *1997 ICIP*, Santa Barbara, CA, vol. 3, pp. 472-475, Oct. 1997.
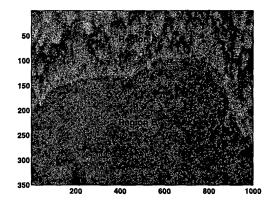
Fig. 1. SAR clutter image with SLICY target in the boundary at column 305.
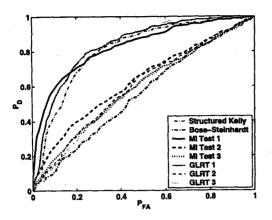
403

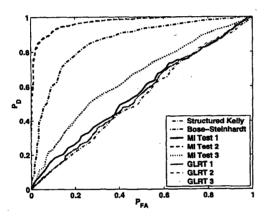**Fig. 2.** ROC curves for Case 1 with SNR = 22dB ($m_A = 50, m_B = 50, n = 51$).

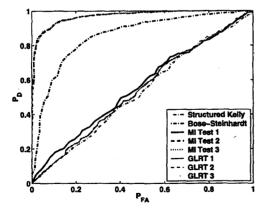**Fig. 3.** ROC curves for Case 2 with SNR = 10dB ($m_A = 40, m_B = 60, n = 61$).

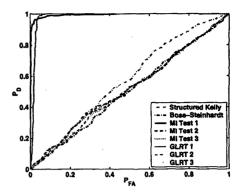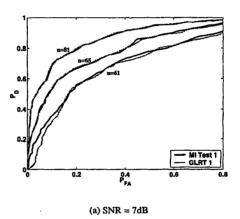**Fig. 4.** ROC curves for Case 3 with SNR = 10dB ($m_A = 40, m_B = 60, n = 61$).

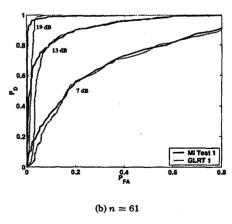**Fig. 5.** ROC curves for Case 1 with SNR = 19dB ($m_A = 60, m_B = 40, n = 61$).

(a) SNR = 7dB

(b) $n = 61$

Fig. 6. Comparison of GLR and MI tests for Case 1 by (a) varying n with fixed SNR and (b) increasing SNR with small n ($m_A = 60, m_B = 40$).
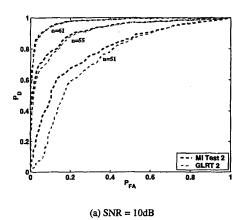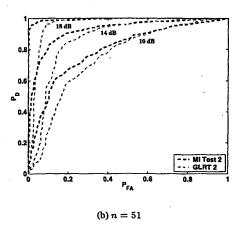
404

Fig. 7. ROC curves for Case 2 with SNR = 10dB (m_A = 50, m_B = 50, n = 61).

(a) SNR = 10dB

(b) n = 51

Fig. 8. Comparison of GLR and MI tests for Case 2 by (a) varying n with fixed SNR and (b) increasing SNR with small n (m_A = 50, m_B = 50).

(a) 142°   (b) 147°   (c) 152°

(d) 157°   (e) 163°   (f) 169°
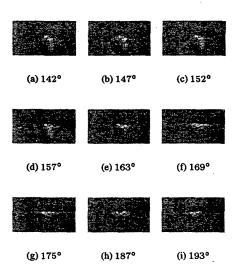
(g) 175°   (h) 187°   (i) 193°

Fig. 9. SLICY canonical target images at elevation 39° and different azimuth angles. Image in (e) is inserted in Fig. 1.

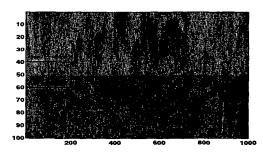**Fig. 10.** Image realigned along the extracted boundary. SLICY target is located at column 305 with $|a|$ = 0.015.
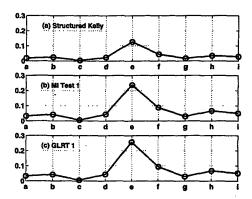
(a) Structured Kelly

(b) MI Test 1

(c) GLRT 1

Fig. 11. Peak values obtained for 9 different target images.

405